View metadata, citation and similar papers at core.ac.uk
brought to you by CORE
provided by Archivio istituzionale della ricerca - Università di Palermo

PHYSICAL REVIEW A **82**, 052313 (2010)

Implementing quantum gates through scattering between a static and a flying qubit

G. Cordourier-Maruri,[1] F. Ciccarello,[2] Y. Omar,[3] M. Zarcone,[2] R. de Coss,[1] and S. Bose[4]
[1]*Departamento de Física Aplicada, Cinvestav-Mérida A.P. 73, Mérida, Yucatán 97310, Mexico*
[2]*CNISM and Dipartimento di Fisica e Tecnologie Relative, Università degli Studi di Palermo, Viale delle Scienze, Edificio 18, I-90128 Palermo, Italy*
[3]*CEMAPRE, ISEG, Universidade Técnica de Lisboa, P-1200-781, and SQIG, Instituto de Telecomunicações, P-1049-001 Lisbon, Portugal*
[4]*Department of Physics and Astronomy, University College London, Gower Street, London WC1E 6BT, United Kingdom*
(Received 27 August 2010; published 15 November 2010)

We investigate whether a two-qubit quantum gate can be implemented in a scattering process involving a flying and a static qubit. To this end, we focus on a paradigmatic setup made out of a mobile particle and a quantum impurity, whose respective spin degrees of freedom couple to each other during a one-dimensional scattering process. Once a condition for the occurrence of quantum gates is derived in terms of spin-dependent transmission coefficients, we show that this can be actually fulfilled through the insertion of an additional narrow potential barrier. An interesting observation is that under resonance conditions this procedure enables a gate only for isotropic Heisenberg (exchange) interactions and fails for an XY interaction. We show the existence of parameter regimes for which gates able to establish a maximum amount of entanglement can be implemented. The gates are found to be robust to variations of the optimal parameters.

DOI: 10.1103/PhysRevA.82.052313 PACS number(s): 03.67.Lx, 03.67.Mn, 03.67.Hk

I. INTRODUCTION

An emerging trend in the quest for viable ways to implement quantum information processing (QIP) tasks [1] is to envisage physical scenarios where the demanded level of control is significantly reduced. A well-known major hindrance to the reliable accomplishment of quantum coherent operations stems from the noise that any required manipulation of quantum "hardware" inevitably introduces whenever a given task is to be achieved. Within this framework, an approach that is becoming increasingly popular is to encode the computational space in the (pseudo-) spin degrees of freedom of scattering particles and harness their interaction during the collision to process quantum information [2–11]. Scattering is indeed a typical phenomenon occurring under low-control conditions: Two or more particles are prepared so as to undergo scattering and eventually measured once this has concluded. Therefore, no direct access to the actual interaction process is available. Unlike gated QIP [1], where one assumes full control over interaction times to implement one- and two-qubit operations, a distinctive feature of scattering-based strategies is that any action is performed with no interaction-time tuning [2–11]. Further advantages of this approach [12] are the remarkable resilience against numerous detrimental effects, such as static disorder and imperfect setting of resonance conditions [5,8,9], detector efficiency [8], and decoherence affecting the centers [6].

Evidently, the price to pay is that in quantum scattering the internal spin degrees of freedom of the scattering particles, that is, those used to encode information, inevitably couple to the motional dynamics. Hence, in general, such processes affect the state of the colliding spins according to quantum maps instead of unitary operations. This makes the accomplishment of QIP tasks, and more in general coherent operations, rather demanding. Indeed, while the works carried out along this line have targeted entanglement generation [2–9] and quantum state tomography [10], only the latest achievements have proved the possibility of performing a quantum *algorithm* such as teleportation [11]. The working principle behind this recent proposal, however, basically relies on a scattering-based effective projective measurement of the singlet state of two remote scattering centers [11], that is, the same basic mechanism underpinning previous works that addressed entanglement generation [5–8].

Our main motivation in the present paper is to assess whether a scattering-based scenario such as the one just depicted can allow for a far more ambitious task: the implementation of a two-qubit gate (TQG). Indeed, while this usually quite demanding quantum operation is well known to be key to build a model for universal quantum computation [1], a scattering scenario appears to be a hostile environment to achieve this because of the nonunitary spin dynamics we have outlined. Aware of such conditions, our main goal in this paper is to provide a proof-of-principle study to establish the possibility of implementing a TQG in a simple paradigmatic model, which can serve as a milestone for forthcoming developments. To tackle the problem, we focus on a setup consisting of a quantum impurity and a mobile particle, the latter being able to propagate along a one-dimensional (1D) wire. We assume a spin-spin Heisenberg-type contact potential such that whenever the particles undergo scattering their spin degrees of freedom mutually interact. As a significant outcome, we show how basic constraints for the occurrence of quantum gates such as linearity and unitarity can be formulated in terms of spin-dependent transmission coefficients through a single, concise, and physically intuitive condition. After showing that this is matched by a rather broad set of parameter patterns, we show that its fulfillment can be given a straightforward explanation in a specific regime on which we will focus for the most part in this paper.

Clearly, assuming monochromatic particles, the detrimental effect of the motional degrees of freedom in the 1D scattering process is to split the spin dynamics into a reflection and a transmission channel. Hence, similar in some respects to other scenarios [13] and in the spirit of the general paradigm

 ©2010 The American Physical Society

of measurement-based quantum computation [14], here our approach is to search for the occurrence of a two-channel probabilistic TQG, that is, a gate that performs one out of two given unitary operations with associated probabilities (i.e., reflectance and transmittance). Although our primary concern is to answer the question whether a TQG can occur regardless of its matrix form, we show that gates that are able to establish maximum entanglement in both the reflection and transmission channels are actually possible under certain conditions.

The present paper is organized as follows. In Sec. II we present the aforementioned setup and briefly discuss the approach that we adopt to describe its scattering dynamics. In Sec. III we derive the condition that must be fulfilled for TQGs to occur. In Sec. IV, focusing on the setting introduced in Sec. II, we illustrate the existence of a regime where that condition holds, and we shed light on the explicit matrix form of the occurring gates. Finally, in Sec. V we discuss the results and draw our conclusions.

II. GENERAL SETUP

We consider a 1D quantum wire along which a flying spin-1/2 particle e can propagate. A quantum impurity $\mathcal{I}$, modeled as a spin-1/2 scatterer, lies at $x = 0$, whereas a narrow potential barrier is located at $x = x_0$ (the x axis is along the wire). The entire setting is sketched in Fig. 1. The Hamiltonian reads as

$$\hat{H} = \frac{\hat{p}^2}{2m} + J\hat{\boldsymbol{\sigma}} \cdot \hat{\boldsymbol{\mathcal{S}}}\delta(x) + \Gamma\delta(x - x_0), \tag{1}$$

where m and $\hat{p}$ are the effective mass and momentum operator of e, respectively, $\hat{\boldsymbol{\sigma}}$ and $\hat{\boldsymbol{\mathcal{S}}}$ are the spin operators of e and $\mathcal{I}$, respectively, J is a spin-spin coupling strength, and Γ is the potential-barrier strength (we set $\hbar = 1$ throughout; note that J and Γ have dimensions of a frequency times a length). Our paradigmatic model naturally fits within solid-state scenarios such as a 1D quantum wire [15] or a single-wall carbon nanotube [16] with an embedded magnetic impurity or quantum dot (see also Ref. [4]). Potential barriers are routinely implemented through applied gate voltages or heterojunctions.

Clearly, because of the spin-spin contact potential [the second term of Hamiltonian (1)], as e enters the interaction region $0 < x < x_0$, scattering along with spin flipping of e and

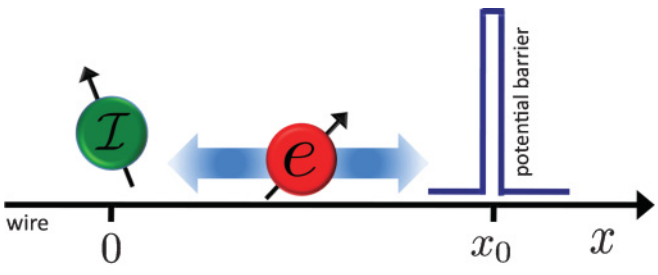

FIG. 1. (Color online) Sketch of the proposed setup for implementing the quantum gate. A mobile particle e can propagate along a wire parallel to the x axis. A quantum impurity $\mathcal{I}$ and a narrow potential barrier lie at $x = 0$ and $x = x_0$, respectively. Once injected into the structure, e undergoes multiple reflections between $\mathcal{I}$ and the potential barrier during which its spin couples to $\mathcal{I}$. Eventually, e is transmitted forward or reflected back.

$\mathcal{I}$ takes place in general. Hence, all the scattering probability amplitudes are spin dependent. As the overall spin space is four-dimensional, the effect of scattering is fully described by two 4×4 matrices whose generic elements read $t_{\alpha,\beta}$ and $r_{\alpha,\beta}$, respectively, where $t_{\alpha,\beta}$ ($r_{\alpha,\beta}$) is the probability amplitude that an initial spin state of the overall system $|\alpha\rangle_{e\mathcal{I}}$ is changed into $|\beta\rangle_{e\mathcal{I}}$ with e being transmitted (reflected). Here $|\alpha\rangle_{e\mathcal{I}}$ and $|\beta\rangle_{e\mathcal{I}}$ are two states of an orthonormal basis spanning the overall spin space.

To derive these matrices, we first observe that according to Eq. (1) the squared total spin of e and $\mathcal{I}$ and its projection along the z axis are conserved quantities, that is, $[\hat{H},\hat{\mathbf{S}}^2] = [\hat{H},\hat{S}_z] = 0$, where $\hat{\mathbf{S}} = \hat{\boldsymbol{\sigma}} + \hat{\mathcal{S}}$ is the total spin. This entails that the dynamics within the singlet and triplet subspaces are decoupled. In each of these subspaces, the spin-spin term of $\hat{H}$ reduces to a spinless potential barrier [17] so that the effective Hamiltonian describes a particle scattering from two spin-independent contact potentials as

$$\hat{H}_S = \frac{\hat{p}^2}{2m} + V_S\,\delta(x) + \Gamma\,\delta(x - x_0), \tag{2}$$

where

$$V_S = \frac{J}{2}\left[S(S+1) - \frac{3}{2}\right] \tag{3}$$

is an effective potential and S is the quantum number associated with $\hat{\mathbf{S}}^2$ so that $S = 0$ ($S = 1$) in the case of the singlet (triplet). By imposing standard boundary conditions on the wave function and its derivative at $x = 0$ and $x = x_0$ [17,18] the transmission and reflection probability amplitudes corresponding to Hamiltonian (2) are straightforwardly calculated as

$$t_S = \frac{4}{4 + 2i\pi\Gamma\rho_\varepsilon + \pi V_S\rho_\varepsilon[2i + (e^{2ikx_0} - 1)\pi\Gamma\rho_\varepsilon]}, \tag{4}$$

$$r_S = \pi\rho_\varepsilon[V_S(\pi\Gamma\rho_\varepsilon - 2i) - \Gamma e^{2ikx_0}(\pi V_S\rho_\varepsilon + 2i)]\frac{t_S}{4}, \tag{5}$$

where $\rho_\varepsilon = (\sqrt{2m/\varepsilon})/\pi\hbar$ is the density of states per unit length [15] of the wire, which is a function of the kinetic energy of e, $\varepsilon = k^2/(2m)$ (k is the wave vector of e). It is straightforward to check that regardless of S the normalization condition is fulfilled, namely,

$$|t_S|^2 + |r_S|^2 = 1. \tag{6}$$

In these calculations, we have used the coupled basis, namely, the common eigenstates of $\hat{\mathbf{S}}^2$ and $\hat{S}_z$, $\mathcal{B} = \{|\Psi^-\rangle_{e\mathcal{I}}, |\uparrow\uparrow\rangle_{e\mathcal{I}}, |\Psi^+\rangle_{e\mathcal{I}}, |\downarrow\downarrow\rangle_{e\mathcal{I}}\}$, where $|m_e = \uparrow,\downarrow\rangle_e$ ($|m_\mathcal{I} = \uparrow,\downarrow\rangle_\mathcal{I}$) are eigenstates of $\hat{\sigma}_z$ ($\hat{\mathcal{S}}_z$) and $|\Psi^\pm\rangle_{e\mathcal{I}} = (|\uparrow\downarrow\rangle_{e\mathcal{I}} \pm |\downarrow\uparrow\rangle_{e\mathcal{I}})/\sqrt{2}$ (henceforth we omit the particle subscripts). As the singlet and triplet spin subspaces are spanned by $|\Psi^-\rangle$ and $\{|\uparrow\uparrow\rangle, |\Psi^+\rangle, |\downarrow\downarrow\rangle\}$, respectively, and the coefficients in Eqs. (4) and (5) depend only on S in the coupled basis $\mathcal{B}$, the transmission and the reflection probability amplitude matrices take a diagonal form:

$$\mathbf{T} = \begin{pmatrix} t_0 & 0 & 0 & 0 \\ 0 & t_1 & 0 & 0 \\ 0 & 0 & t_1 & 0 \\ 0 & 0 & 0 & t_1 \end{pmatrix} \tag{7}$$

(an analogous expression having the transmission coefficients replaced with the reflection ones holds for the reflection-probability-amplitude matrix $\mathbf{R}$).

III. CONDITION FOR THE OCCURRENCE OF QUANTUM GATES

In general, because of the coupling between the spin and motional degrees of freedom during scattering, neither $\mathbf{T}$ nor $\mathbf{R}$ represents a unitary operator within the overall spin space. Rather, they are the matrix representations of two Kraus operators, which because of the normalization condition (6) fulfill the equation

$$\mathbf{T}\,\mathbf{T}^\dagger + \mathbf{R}\mathbf{R}^\dagger = \mathbb{1}_4, \tag{8}$$

where $\mathbb{1}_4$ is the 4×4 identity matrix. For the transmission channel, the initial spin density matrix ρ transforms into ρ' after scattering:

$$\rho' = \frac{\mathbf{T}\rho\,\mathbf{T}^\dagger}{P_t}, \tag{9}$$

where

$$P_t = \mathrm{Tr}[\mathbf{T}\rho\,\mathbf{T}^\dagger] \tag{10}$$

is the overall transmission probability (analogous equations hold for the reflection channel). Because of the denominator (10), Eq. (9) shows that $\mathbf{T}$ and $\mathbf{R}$, in general, act in a nonlinear way, which would rule out the fulfillment of another essential requirement for a gate: linearity. One may wonder, however, whether a *specific* regime exists in the setup described in Sec. II such that unitarity and linearity occur together, a circumstance that we will show actually takes place. To this aim we consider the explicit form of the transmittivity P_t in Eq. (10), which reads as

$$P_t = |t_0|^2\rho_- + |t_1|^2(\rho_{\uparrow\uparrow} + \rho_+ + \rho_{\downarrow\downarrow}), \tag{11}$$

where $\rho_\alpha = \langle\alpha|\rho|\alpha\rangle$ ($\alpha = \uparrow\uparrow, \downarrow\downarrow$) and $\rho_\pm = \langle\Psi^\pm|\rho|\Psi^\pm\rangle$ (an analogous expression clearly holds for the reflection channel). It is now straightforward to see that because of normalization of the initial spin state, that is, $\mathrm{Tr}\rho = 1$, when

$$|t_0| = |t_1|, \tag{12}$$

P_t does not depend on ρ so as to make the map (9) linear. Furthermore, using Eq. (6) we see that in such a case $|r_0| = |r_1|$ is fulfilled as well. In this regime, once rescaled operators are defined as $\tilde{\mathbf{T}} = \mathbf{T}/|t_0|$ and $\tilde{\mathbf{R}} = \mathbf{R}/|r_0|$, the spin state evolves in the transmission (reflection) channel as $\rho' = \tilde{\mathbf{T}}\rho\tilde{\mathbf{T}}^\dagger$ ($\rho' = \tilde{\mathbf{R}}\rho\tilde{\mathbf{R}}^\dagger$). We can immediately check that

$$\tilde{\mathbf{T}}\,\tilde{\mathbf{T}}^\dagger = \tilde{\mathbf{T}}^\dagger\,\tilde{\mathbf{T}} = \tilde{\mathbf{R}}\,\tilde{\mathbf{R}}^\dagger = \tilde{\mathbf{R}}^\dagger\,\tilde{\mathbf{R}} = \mathbb{1}_4; \tag{13}$$

that is, both $\tilde{\mathbf{T}}$ and $\tilde{\mathbf{R}}$ are unitary.

Summarizing, we have found that the simple condition (12) is enough to ensure both linearity and unitarity of the transmission and reflection channels. This indeed has a reasonable interpretation because of the implicit requirement that, clearly, to implement a quantum gate a mere path measurement over e must provide zero information about the overall spin state of e and $\mathcal{I}$. It is also clear that this takes place provided that for each state of a given basis, such as $\mathcal{B}$, the mobile particle is transmitted (reflected) with the same probability (and hence it happens thus for any spin state), a circumstance that, looking at Eq. (7), we see to be equivalent to condition (12).

We are now in a position to justify why our setup in Fig. 1 includes a static potential barrier $\Gamma\delta(x - x_0)$ [see Sec. II and Eq. (1)]. In the absence of this barrier, that is, when $\Gamma = 0$, Eq. (2) shows that within the singlet (triplet) subspace the effective Hamiltonian would be that of a particle e scattering from a single delta-like potential barrier $-3/4J\delta(x)$ [$J/4\,\delta(x)$]. For a particle scattered by a potential $V\delta(x)$, a straightforward calculation gives that the transmission and reflection probability amplitudes $t(V)$ and $r(V)$ are given by

$$t(V) = 1 - r(V) = \frac{4}{4 + 2i\pi\rho_\varepsilon V}, \tag{14}$$

a result that can also be obtained as a special case of Eq. (4). It is now clear that without additional scatterers there is no way to fulfill Eq. (12) since $|t(-3/4J)| \neq |t(J/4)|\ \forall J$, which means that no quantum gate is possible with the simple setting consisting of e and $\mathcal{I}$. In the next section, we will clearly elucidate the mechanism through which the static barrier compensates for this drawback.

We conclude this section by showing what class of quantum gates can be implemented by virtue of Eq. (12). Because this requires that the transmittivity (reflectivity) needs to be the same in the singlet and triplet subspaces, the only effect of scattering is to give rise to a relative phase shift. Therefore, in the coupled basis $\mathcal{B}$ the general form of the gate compatible with Eq. (12) reads as

$$\tilde{\mathbf{T}} = \begin{pmatrix} e^{i\varphi_t} & 0 & 0 & 0 \\ 0 & 1 & 0 & 0 \\ 0 & 0 & 1 & 0 \\ 0 & 0 & 0 & 1 \end{pmatrix}, \tag{15}$$

where $\varphi_t = \arg t_0 - \arg t_1$. In the computational basis $\mathcal{B}' = \{|\uparrow\uparrow\rangle, |\uparrow\downarrow\rangle, |\downarrow\uparrow\rangle, |\downarrow\downarrow\rangle\}$ (we encode the two qubit logical states $|0\rangle$ and $|1\rangle$ into $|\uparrow\rangle$ and $|\downarrow\rangle$, respectively) the gate has the general matrix representation

$$\tilde{\mathbf{T}}' = \begin{pmatrix} 1 & 0 & 0 & 0 \\ 0 & \frac{1+e^{i\varphi_t}}{2} & \frac{1-e^{i\varphi_t}}{2} & 0 \\ 0 & \frac{1-e^{i\varphi_t}}{2} & \frac{1+e^{i\varphi_t}}{2} & 0 \\ 0 & 0 & 0 & 1 \end{pmatrix}. \tag{16}$$

Analogous arguments hold for the reflection channel. Later we discuss the entangling power of the class of gates (16).

IV. IMPLEMENTING THE QUANTUM GATE

We now show the existence of parameter patterns such that the setup in Fig. 1 behaves so as to satisfy Eq. (12). We recall that according to Hamiltonian (1) the system dynamics depends on the three dimensionless parameters $\rho_\varepsilon J$, $\rho_\varepsilon\Gamma$, and kx_0 (see Sec. II). In Fig. 2 we set three different ratios between Γ and J. For each of these, we plot $|t_0| - |t_1|$ against kx_0 for different values of $\rho_\varepsilon J$. First, note that for assigned values of Γ/J and $\rho_\varepsilon J$ the plots are periodic in kx_0 with period π, in

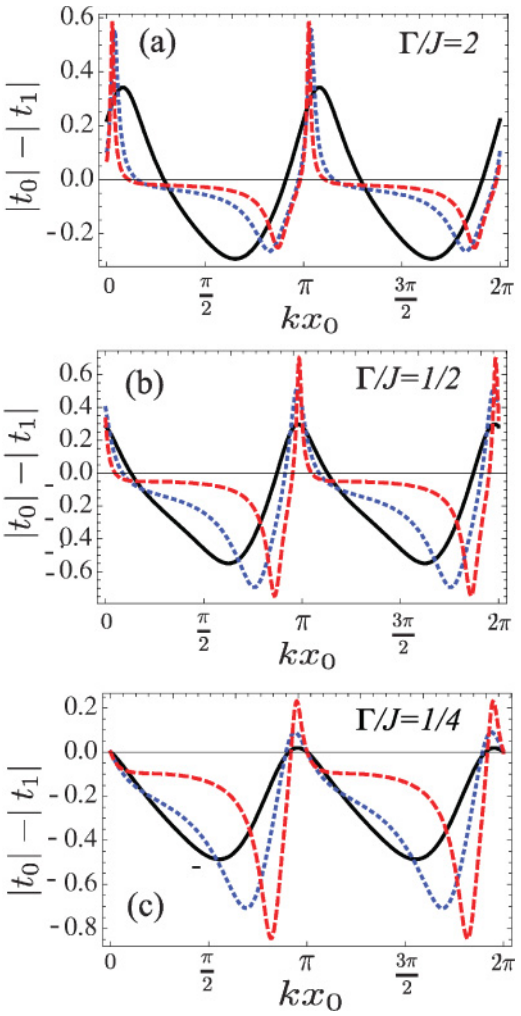

FIG. 2. (Color online) $|t_0| - |t_1|$ vs kx_0 (dimensionless) for various settings of Γ/J and $\rho_\varepsilon J$. (a) $\Gamma/J = 2$ and $\rho_\varepsilon \Gamma = 0.5$ (black solid line), 2 (blue dotted line), and 3 (red dashed line). (b) $\Gamma/J = 1/2$ and $\rho_\varepsilon \Gamma = 1$ (black solid line), 2 (blue dotted line), and 4 (red dashed line). (c) $\Gamma/J = 1/4$ and $\rho_\varepsilon \Gamma = 1$ (black solid line), 2 (blue dotted line), and 4 (red dashed line).

agreement with Eqs. (4) and (5). As is evident, condition (12) occurs in each case addressed in Fig. 2 whenever the plotted curves intersect the kx_0 axis. Remarkably, when $\Gamma/J = 1/4$ [see Fig. 2(c)] provided that $kx_0 = n\pi$ ($n \in \mathbb{N}$) the condition for the occurrence of quantum gates is satisfied regardless of $\rho_\varepsilon J$, which is of course an attractive feature for the demand of low control. Insight into this phenomenon can be given through a simple line of reasoning as follows.

Under the resonance conditions (RCs) $kx_0 = n\pi$ the effective representations of the two Dirac δ functions appearing in Eq. (1) coincide according to the equation

$$\delta_{\mathrm{RC}}(x) = \delta_{\mathrm{RC}}(x - x_0), \tag{17}$$

where the subscripts are a reminder that these are effective forms under RCs (for a proof see Refs. [4,6], where an analogous effect has been shown to be useful for QIP tasks). Hence, in light of Eq. (17) under RCs the system behaves as if the static potential lay at the site of $\mathcal{I}$. In such a case, using Eqs. (2) and (3) the effective potentials for $S = 0,1$ become $(\Gamma - 3/4J)\delta_{\mathrm{RC}}(x)$ and $(\Gamma + J/4)\delta_{\mathrm{RC}}(x)$, respectively. As we have already shown (see the previous section), when $\Gamma = 0$, such single-barrier potentials necessarily entail that $|t_0| \neq |t_1|$ according to Eq. (14). When $\Gamma \neq 0$, however, a closer inspection of Eq. (14) shows that for a single δ-like barrier $V\delta(x)$ the modulus of the transmission coefficient depends only on $|V|$. Hence, Eq. (12) is fulfilled when

$$\Gamma - \frac{3}{4}J = -\left(\Gamma + \frac{J}{4}\right), \tag{18}$$

which is indeed equivalent to $\Gamma/J = 1/4$ regardless of $\rho_\varepsilon J$ and thus explains the behavior in Fig. 2(c). A more explicit and illustrative way to see this is noting that under RCs the effective Hamiltonian can be arranged as

$$\hat{H} = \frac{\hat{p}^2}{2m} + J\left(\frac{\Gamma}{J} + \hat{\sigma}_z\hat{S}_z + \frac{\hat{\sigma}_+\hat{S}_- + \hat{\sigma}_-\hat{S}_+}{2}\right)\delta_{\mathrm{RC}}(x). \tag{19}$$

When the initial spin state is $|\uparrow\uparrow\rangle$ or $|\downarrow\downarrow\rangle$ the factor between the parentheses takes the value $\Gamma/J + 1/4$, which results in the effective potential-barrier height $\Gamma + J/4$. On the other hand, $|\Psi^\pm\rangle$ fulfill the equations

$$\hat{\sigma}_z\hat{S}_z|\Psi^\pm\rangle = -\frac{1}{4}|\Psi^\pm\rangle, \tag{20}$$

$$\frac{\hat{\sigma}_+\hat{S}_- + \hat{\sigma}_-\hat{S}_+}{2}|\Psi^\pm\rangle = \pm\frac{1}{2}|\Psi^\pm\rangle. \tag{21}$$

It is now easy to see that the static barrier, whose presence is embodied by the constant term Γ/J between the parentheses in Eq. (19), in fact cancels out the Ising term for $\Gamma/J = 1/4$. When this takes place, the effective potential-barrier height seen by $|\Psi^\pm\rangle$ becomes $\pm J/2$, whose modulus is the same as the one associated with $|\uparrow\uparrow\rangle$ and $|\downarrow\downarrow\rangle$. This line of reasoning also shows, in particular, that the replacement of a Heisenberg-type spin-spin coupling with an XY-isotropic one in the Hamiltonian (1) cannot give rise to any quantum gate, either with no extra barriers or with a δ-like barrier under RCs. Indeed, in the Heisenberg case one deals with only two independent transmission coefficients (t_0 and t_1), and hence the single condition (12) needs to be fulfilled to implement gates. In the XY-isotropic model, however, *three* independent coefficients in general arise since the spin-spin scattering potential vanishes for both $|\uparrow\uparrow\rangle$ and $|\downarrow\downarrow\rangle$ and takes the effective value $\pm J/2$ for $|\Psi^\pm\rangle$ [see Eq. (21)]. In light of our discussion in Sec. III, we see that in the case of the XY-isotropic model, the gates' occurrence gives two equations to be fulfilled. Absence of gates under RCs with such a model is therefore not surprising given that setting RCs in fact freezes the parameter kx_0: Judicious setting of the remaining free parameter Γ is enough to fulfill the single equation required by the Heisenberg model, but not the two met in the presence of XY-isotropic coupling.

Having identified a regime compatible with Eq. (12), our next task is to illustrate what specific forms of $\tilde{\mathbf{T}}'$ and $\tilde{\mathbf{R}}'$ can occur within the general family in Eq. (16), which is in fact equivalent to exploring what values φ_t and φ_r can take.

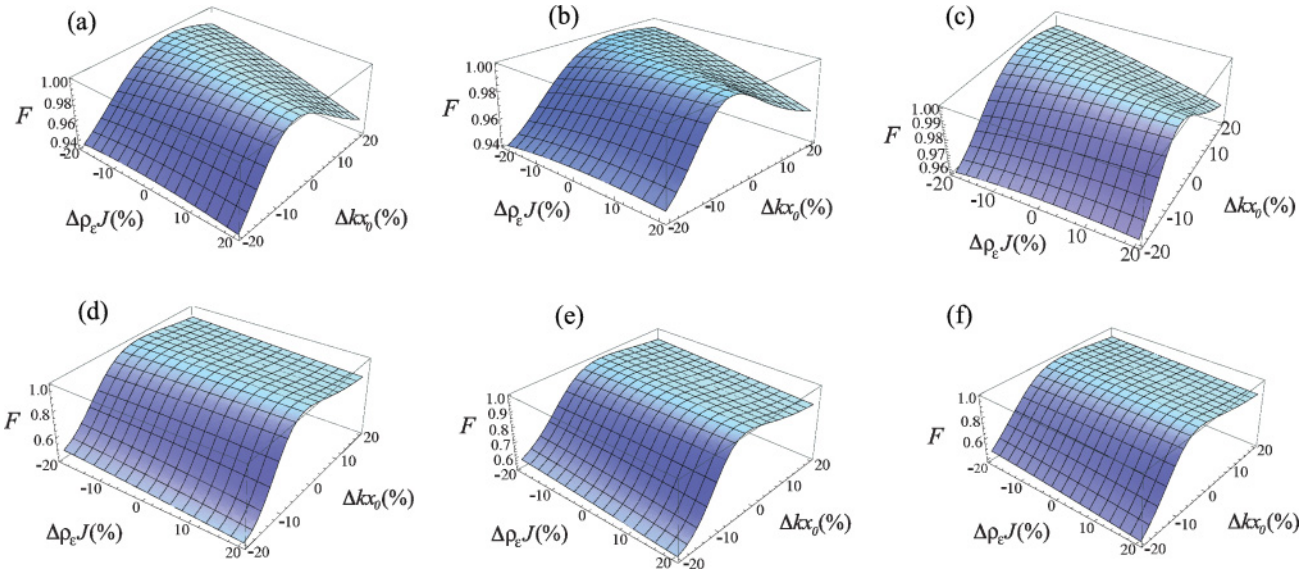

FIG. 3. (Color online) Fidelity F vs the percentage deviations from the ideal values $\Delta\rho_\varepsilon J$ and Δkx_0 for the initial spin states $|\uparrow\downarrow\rangle$ [(a) and (d)], $(|\uparrow\uparrow\rangle + |\downarrow\downarrow\rangle + |\uparrow\downarrow\rangle - |\downarrow\uparrow\rangle)/2$ [(b) and (e)], and $(|\uparrow\rangle + |\downarrow\rangle) \bigotimes (|\uparrow\rangle + i|\downarrow\rangle)/2$ [(c) and (f)]. Plots (a), (b), and (c) refer to the transmission-channel gate, whereas (d), (e), and (f) refer to the reflection-channel gate.

In the regime $\Gamma/J = 1/4$ and $kx_0 = n\pi$, a straightforward calculation along with use of Eqs. (3) and (14) yields

$$\varphi_t = 2\arctan\frac{\pi\rho_\varepsilon J}{4}, \tag{22}$$

$$\varphi_r = -2\arctan\frac{4}{\pi\rho_\varepsilon J} + 2\pi. \tag{23}$$

In light of Eqs. (16), (22) and (23) fully specify the form taken by gates $\tilde{\mathbf{T}}'$ and $\tilde{\mathbf{R}}'$ in the regime $\Gamma/J = 1/4$ and $kx_0 = n\pi$. Thus both phase shifts φ_t and φ_r grow with $\rho_\varepsilon J$ tending to an asymptotic value, which is π in the case of φ_t and 2π in the case of φ_r (for any $\rho_\varepsilon J$ we have $\varphi_t - \varphi_r = \pi$).

A question that is naturally raised from the matrix structure in Eq. (16) is whether the elements of the central 2×2 block can all have the same modulus. Indeed, in such a case the gate is clearly able to establish *maximum entanglement*. It is easy to see that this circumstance occurs provided that $|1 + e^{i\varphi_t}| = |1 - e^{i\varphi_t}|$, which requires $\cos\varphi_t = 0$ and hence $\varphi_t = (2q+1)\pi/2$, where $q \in \mathbb{Z}$ (analogous arguments hold true for the reflection channel). In our case, using Eqs. (22) and (23), we obtain $\varphi_t = \varphi_r - \pi = \pi/2$ for $\rho_\varepsilon J = 4/\pi \simeq 1.27$, which entails the gate matrix form

$$\mathbf{U} = \begin{pmatrix} 1 & 0 & 0 & 0 \\ 0 & \frac{1\pm i}{2} & \frac{1\mp i}{2} & 0 \\ 0 & \frac{1\mp i}{2} & \frac{1\pm i}{2} & 0 \\ 0 & 0 & 0 & 1 \end{pmatrix}, \tag{24}$$

where the $+$ $(-)$ sign holds for the transmission (reflection) channel. Also, using Eqs. (3) and (14), we can easily check that in such a case $|t_0| = |t_1| = |r_0| = |r_1| = 1/2$, namely, that the success probabilities associated with the reflection and transmission gates are the same. We have thus found a parameter pattern such that gates able to create maximum entanglement occur in both the reflection and transmission channels. Taking, for instance, the initial product state $|\uparrow\downarrow\rangle$ we obtain that, up to an irrelevant phase factor, $\hat{U}|\uparrow\downarrow\rangle = (|\uparrow\downarrow\rangle \mp i|\downarrow\uparrow\rangle)/\sqrt{2}$, where the $-$ $(+)$ sign holds for the transmission (reflection) channel.

As we have proved, for our setup to implement gates, certain parameter values need to be set. This feature may appear somewhat unnatural in the low-control scattering scenario that we have considered. A legitimate question is therefore how robust the gate is to an imperfect setting of the ideal parameters. To answer this, we consider the paradigmatic situation where one wishes to implement the maximally entangling gate (24), which requires us to set $\Gamma/J = 1/4$, $\rho_\varepsilon J = 4/\pi$, and $kx_0 = n\pi$. To measure how well such a gate is implemented for an imperfect matching of this ideal pattern we use quantum fidelity [1]. Specifically, for a given initial pure spin state $\rho = |\Psi_i\rangle\langle\Psi_i|$ we compute the fidelity F between the output state ρ' as given in Eq. (9) (in general this is mixed) and the output state $|\Psi_f\rangle = \hat{U}|\Psi_i\rangle$ that would be obtained in the ideal case. The expression of fidelity is $F = \langle\Psi_f|\rho'|\Psi_f\rangle$. In Fig. 3, we have carried out this study for the transmission and reflection channels [Figs. 3(a)–3(c) and 3(d)–3(f), respectively] and the three representative initial states $|\uparrow\downarrow\rangle$, $(|\uparrow\uparrow\rangle + |\downarrow\downarrow\rangle + |\uparrow\downarrow\rangle - |\downarrow\uparrow\rangle)/2$, and $(|\uparrow\rangle + |\downarrow\rangle) \bigotimes (|\uparrow\rangle + i|\downarrow\rangle)/2$. In each case, we set the condition $\Gamma/J = 1/4$ and plot F against $\Delta\rho_\varepsilon J$ and Δkx_0, where $\Delta\rho_\varepsilon J$ (Δkx_0) is the percentage difference between $\rho_\varepsilon J$ (kx_0) and the corresponding ideal value. As is evident in the plots, the robustness of the transmission-channel gate is quite striking. For deviations from the ideal values up to 20%, in the worst case F slightly decreases to $\simeq 0.94$. On the other hand, the reflection channel exhibits generally lower performance [19], especially for negative values of Δkx_0. In this channel, however, for $|\Delta kx_0|$ up to $\simeq 8\%$ F exceeds 0.9.

Such generally good resilience is in line with the outcomes of analogous tests in similar setups [5,8,9], which further confirms a major advantage of scattering-based methods in accomplishing QIP tasks (see the introduction).

V. CONCLUSIONS

In this work we have tackled the issue whether a TQG can be implemented in a setup made out of mobile and static qubits undergoing quantum scattering processes. Despite the many advantages of such a scattering scenario for QIP purposes [2–11] and the well-known importance of TQGs [1], this question had so far remained fully unanswered in the literature. With these motivations in mind, we have considered a minimal paradigmatic setup comprising a flying spin scattering from a quantum impurity along with a further spinless potential barrier. In a way similar to other scenarios where proposals for probabilistic quantum gates were put forward [13] we have assessed whether a unitary transformation in the overall spin space can be probabilistically implemented in each of the transmission and reflection channels. By imposing basic constraints such as linearity and unitarity, we have found that gates occur in both channels provided that a simple and physically intuitive condition is obeyed. We have also given the full class of resulting gates. Next, numerical evidence has been given that this theoretical condition is actually matched for suitable parameter patterns in both off-resonance and resonance conditions. After focusing on RCs, we have analytically derived the exact parameter pattern that ensures the occurrence of gates. Insight into the related underlying mechanism has been given by explaining, in particular, the essential role played by the additional potential barrier. Among the possible occurring gates, we have identified one able to establish maximum entanglement and have given the exact required parameter setting. Finally, we have shown that such a maximally entangling gate is robust against imperfect matching of the optimal parameters.

As anticipated, a significant implication of our findings is the ability of certain occurring gates to establish maximum entanglement. Entanglement between a static and a flying qubit offers the major advantage of being particularly prone to a robust Bell test since once scattering has happened the two particles can get significantly far apart from each other.

In this work, we have mainly focused on achieving gates under RCs. Indeed, this regime is more prone to analytical treatment than the more general off-resonance case. This enabled us to highlight numerous key issues without mathematical hindrances. However, as we have seen, even off-resonance conditions allow for occurrence of TQGs. A comprehensive study of this case, which goes beyond the scope of this paper, is therefore highly desirable and will be the subject of a future publication [20].

The entanglement between a static ionic and a flying photonic qubit has been envisaged for connecting ion-trap quantum registers [21]. Likewise, it is quite possible that the scheme we propose here will open up scaling opportunities for spin-based quantum computation in solid-state systems [22].

ACKNOWLEDGMENTS

Fruitful discussions with D. E. Browne are gratefully acknowledged. Y.O. thanks support from project IT-QuantTel, as well as from Fundação para a Ciência e a Tecnologia (Portugal), through programs POCTI/POCI/PTDC and project PTDC/EEA-TEL/103402/2008 QuantPrivTel, partially funded by FEDER (EU). G.C. and R.C. thank the Department of Physics and Astronomy, University College London, and SQIG, Instituto de Telecomunicações, for their hospitality as well as financial support from CONACYT (Mexico) under Grant No. 83604.

[1] M. A. Nielsen and I. L. Chuang, *Quantum Computation and Quantum Information* (Cambridge University Press, Cambridge, UK, 2000).

[2] A. M. Childs, Phys. Rev. Lett. **102**, 180501 (2009); T. Zibold, P. Vogl, and A. Bertoni, Phys. Rev. B **76**, 195301 (2007); A. E. Popescu and R. Ionicioiu, *ibid.* **69**, 245422 (2004); A. Bertoni, P. Bordone, R. Brunetti, C. Jacoboni, and S. Reggiani, Phys. Rev. Lett. **84**, 5912 (2000).

[3] A. T. Costa Jr., S. Bose, and Y. Omar, Phys. Rev. Lett. **96**, 230501 (2006); G. L. Giorgi and F. de Pasquale, Phys. Rev. B **74**, 153308 (2006); K. Yuasa and H. Nakazato, J. Phys. A: Math. Theor. **40**, 297 (2007); Y. Hida, H. Nakazato, K. Yuasa, and Y. Omar, Phys. Rev. A **80**, 012310 (2009).

[4] F. Ciccarello *et al.*, New J. Phys. **8**, 214 (2006); J. Phys. A: Math. Theor. **40**, 7993 (2007); F. Ciccarello, G. M. Palma, and M. Zarcone, Phys. Rev. B **75**, 205415 (2007); F. Ciccarello, M. Paternostro, G. M. Palma, and M. Zarcone, *ibid.* **80**, 165313 (2009).

[5] F. Ciccarello, M. Paternostro, M. S. Kim, and G. M. Palma, Phys. Rev. Lett. **100**, 150501 (2008).

[6] F. Ciccarello, M. Paternostro, G. M. Palma, and M. Zarcone, New J. Phys. **11**, 113053 (2009).

[7] K. Yuasa, J. Phys. A **43**, 095304 (2010).

[8] K. Yuasa, D. Burgarth, V. Giovannetti, and H. Nakazato, New J. Phys. **11**, 123027 (2009).

[9] F. Ciccarello *et al.*, Las. Phys. **17**, 889 (2007); F. Ciccarello, M. Paternostro, M. S. Kim, and G. M. Palma, Int. J. Quantum Inform. **6**, 759 (2008).

[10] A. de Pasquale, K. Yuasa, and H. Nakazato, Phys. Rev. A **80**, 052111 (2009).

[11] F. Ciccarello, S. Bose, and M. Zarcone, Phys. Rev. A **81**, 042318 (2010).

[12] In this work, in contrast to the authors of Ref. [2], we focus on the scattering-based QIP paradigm, which exploits scattering centers possessing internal spin degrees of freedom [3–11]. In the remainder of the paper, it is therefore the latter scenario that we have in mind when using the term "scattering."

[13] Y. L. Lim, A. Beige, and L. C. Kwek, Phys. Rev. Lett. **95**, 030505 (2005); D. Gross, K. Kieling, and J. Eisert, Phys. Rev. A **74**, 042343 (2006); P. Kok *et al.*, Rev. Mod. Phys. **79**, 135 (2007); H. Goto and K. Ichimura, Phys. Rev. A **80**, 040303 (2009).

[14] H. J. Briegel, D. E. Browne, W. Dür, R. Raussendorf, and M. Van den Nest, Nat. Phys. (London) **5**, 19 (2009).

[15] J. H. Davies, *The Physics of Low-Dimensional Semiconductors: An Introduction* (Cambridge University Press, Cambridge, UK, 1998).

[16] S. J. Tans, M. H. Devoret, H. Dai, H. A. Thess, R. E. Smalley, L. J. Geerligs, and C. Dekker, Nature (London) **386**, 474 (1997).

[17] O. L. T. de Menezes and J. S. Helman, Am. J. Phys. **53**, 1100 (1984); W. Kim, R. K. Teshima, and F. Marsiglio, Europhys. Lett. **69**, 595 (2005).

[18] J.-B. Xia, Phys. Rev. B **45**, 3593 (1992).

[19] This is due to the low associated reflection probability. Indeed, the setting $\rho_\varepsilon J = 4/\pi, \Gamma/J = 1/4$, and $kx_0 = n\pi$ yields $|t_0|^2 = |t_1|^2 = 0.908$ and $|r_0|^2 = |r_1|^2 = 0.092$, where we have used Eqs. (4) and (6). Equation (6) also shows that $||t_0|^2 - |t_1|^2| = ||r_0|^2 - |r_1|^2|$. An imperfect setting of RCs thus causes the same absolute discrepancies between $|\eta_0|^2$ and $|\eta_1|^2$ ($\eta = r,t$) in the two channels. However, because the reflection coefficients under RCs are small, the *relative* discrepancy will be higher for them. Hence, violation of Eq. (12) is more significant for the reflection channel than for the transmission channel.

[20] G. Cordourier-Maruri *et al.* (unpublished).

[21] B. B. Blinov and D. L. Moehring, L. M. Duan, and C. Monroe, Nature (London) **428**, 153 (2004).

[22] D. D. Awschalom, D. Loss, and N. Samarth, *Semiconductor Spintronics and Quantum Computation* (Springer, Berlin, 2002).